Available online at www.sciencedirect.com

ScienceDirect

International Journal of Heat and Mass Transfer 50 (2007) 3054–3061

International Journal of HEAT and MASS TRANSFER

www.elsevier.com/locate/ijhmt

Determination of thermal conductivity and emissivity of electromagnetically levitated high-temperature droplet based on the periodic laser-heating method: Theory

Takao Tsukada [a,*], Hiroyuki Fukuyama [b], Hidekazu Kobatake [b]

[a] *Department of Chemical Engineering, Osaka Prefecture University, 1-1 Gakuen-cho, Naka-ku, Sakai, Osaka 599-8531, Japan*
[b] *Institute of Multidisciplinary Research for Advanced Materials, Tohoku University, 2-1-1 Katahira, Aoba-ku, Sendai 980-8577, Japan*

Received 8 May 2006; received in revised form 13 November 2006
Available online 13 March 2007

Abstract

Recently, a novel method of measuring the thermophysical properties, especially thermal conductivity, of high-temperature molten materials using the electromagnetic levitation technique has been developed by [H. Fukuyama, H. Kobatake, I. Minato, K. Takahashi, T. Tsukada, S. Awaji, Establishment of noncontact AC calorimetry of high-temperature melts using solid platinum spheres as a reference, in: Proceedings of 16th Symposium on Thermophysical Properties, CD-ROM, 2006, p. 937; H. Kobatake, H. Fukuyama, I. Minato, T. Tsukada, S. Awaji, Noncontact AC calorimetry of liquid silicon with suppressing convections in a static magnetic field, in: Proceedings of 16th Symposium on Thermophysical Properties, CD-ROM, 2006, p. 625], where the method was based on periodic laser-heating, and a static magnetic field was superimposed to suppress convection in an electromagnetically levitated droplet. In the present work, the periodic laser-heating method was modeled to estimate the thermal conductivity and emissivity of the electromagnetically levitated droplet using a measured parameter, i.e., the phase lag between the modulated light and the temperature variations detected by a pyrometer, $\Delta\phi_s$, at various frequencies of the modulated light ω. Here, the unsteady-state heat conduction equation for the droplet accompanying radiative heat transfer to the ambient was simplified and transformed to steady-state linear equations. The experimental relation between $\Delta\phi_s$ and ω was fitted by the mathematical model proposed here to estimate simultaneously the thermal conductivity and emissivity of molten silicon. Also, the numerical simulations for unsteady thermal field in the electromagnetically levitated droplet which was periodically laser-heated were carried out to demonstrate the validity of the proposed simplified model, and then to investigate the sensitivity of the thermophysical properties to the relation between $\Delta\phi_s$ and ω.

Keywords: Thermal conductivity; Emissivity; Electromagnetic levitation; Static magnetic field; Periodic laser-heating method; Theory

1. Introduction

Modern information technology (IT), which requires high-speed data processing and high-speed data transmission, is supported by high-quality and large semiconductor, silicon crystals. Silicon crystals are mostly grown by the Czochralski (CZ) method, one of the methods for producing single crystals from the melt. Because the melt flow and other transport phenomena in the CZ furnace affect strongly the shape of the melt/crystal interface, the distributions of the temperature, oxygen concentration and point defects in the crystal, and consequently the crystal quality, it is very important to have a clear understanding of the physical processes in the CZ furnace in order to produce high-quality silicon single crystals efficiently and economically. The silicon crystal diameter is increasing markedly from 8 to 12 in. nowadays and to 16 inches in the near future, and consequently the melt convection behavior becomes very complicated, i.e., turbulent and oscillatory. Therefore, the experimental investigations of

* Corresponding author. Tel.: +81 72 254 9302; fax: +81 72 254 9911.
E-mail address: tsukada@chemeng.osakafu-u.ac.jp (T. Tsukada).

0017-9310/$ - see front matter
doi:10.1016/j.ijheatmasstransfer.2006.12.026

Nomenclature

C_p	specific heat (J/kg K)
$\boldsymbol{e}_{\mathrm{laser}}$	unit vector pointing out the incident direction of laser beam
I_0	laser intensity at the centerline (W/m^2)
k	thermal conductivity (W/m K)
n	normal distance from the droplet surface
$\boldsymbol{n}$	unit normal vector at the droplet surface
P_0	laser power (W)
Q	heat generation rate (W/m^3)
R_{s}	radial distance of droplet surface (m)
r	radial distance in spherical coordinates (m)
r_{laser}	e^{-2} radius of laser beam (m)
$S_{\mathrm{pyrometer}}$	spot area of pyrometer (m^2)
T	temperature (K)
T_0	initial temperature (K)
T_{a}	ambient temperature (K)
ΔT_{av}	average temperature (K)
ΔT_{md}	modulation amplitude (K)
t	time (s)
x, y and z	each distance in Cartesian coordinates (m)
α	absorptivity (–)
ε	emissivity (–)
ϕ	azimuthal angle in spherical coordinates (rad)
$\Delta\phi_{\mathrm{s}}$	phase lag (deg)
θ	polar angle in spherical coordinates (rad)
ρ	density (kg/m^3)
σ_{SB}	Stefan–Boltzmann constant (W/m^2 K^4)
ω	frequency of modulated laser beam (rad/s)

Superscripts

in	in-phase component
out	out-of-phase component

the phenomena in the melt are not so easy, and thus many numerical studies have been carried out to explore the melt convection in the real crystal growth process [1–3].

To obtain accurate results by numerical simulation, the precise thermophysical properties that serve as the input data of the simulation are absolutely necessary as well as the elaborate mathematical model, such as the appropriate turbulence model for melt convection in a large crucible. However, it is difficult to measure the thermophysical properties of molten silicon because of its high melting point temperature and high reactivity, and consequently contamination from the container wall. Recently, the precise measurement of the thermophysical properties of molten silicon, such as density, surface tension, and viscosity, has been carried out using the electromagnetic and electrostatic levitation technique under both terrestrial and microgravity conditions [4–13], since they allow the properties to be measured precisely over a wide temperature range including the undercooled condition without contamination. However, even using the electromagnetic levitation technique, measuring precisely the thermal conductivity of molten silicon has still been considered to be difficult, because convection driven by the buoyancy force, thermocapillary force due to the temperature dependence of the surface tension on the melt surface, and electromagnetic force to levitate the molten silicon droplet strongly affects the measurement of thermal conductivity. In particular, it is well-known that the flow velocity of the magnetohydrodynamic (MHD) convection induced by the electromagnetic force reaches 10–40 cm/s [14–17]. This means that the measured value is an effective thermal conductivity contributed by convective heat transfer in addition to conduction. Although such a strong MHD convection might be suppressed in a microgravity environment because of the much smaller lifting force of sample, we can seldom have a chance to measure the thermal conductivity of the molten silicon under microgravity.

Recently, Fukuyama et al. [18,19] have developed a novel method of measuring the thermal conductivity, specific heat and emissivity of molten material using the electromagnetic levitation technique, where the method was based on periodic laser-heating and a static magnetic field was superimposed to suppress melt convection in an electromagnetically levitated droplet, as shown in Fig. 1. Using the electromagnetic levitator installed inside a superconducting magnet, a molten silicon droplet was heated and levitated, and additionally convection in the droplet was suppressed by the Lorentz force due to the interaction between the electrically conductive fluid flow and the static magnetic field. This technique can allow us to measure stably thermophysical properties other than these, such as density and surface tension, over a wide temperature range including the undercooled condition without any possible contamination. In this paper, the mathematical model proposed to determine simultaneously the thermal conductivity and emissivity of an electromagnetically levitated droplet, using an electromagnetic levitator with a static magnetic field, is presented in detail. The specific heat of the droplet, which is needed to determine the thermal conductivity, can be separately measured with the same electromagnetic levitator, being based on ac calorimetry. The details of specific heat measurement are described in Ref. [18].

2. Model formulations and methodology

2.1. Governing equations and boundary conditions

Fig. 2 shows a schematic diagram of a periodic laser-heating method. The upper part of an electromagnetically levitated droplet is periodically heated by a modulated light

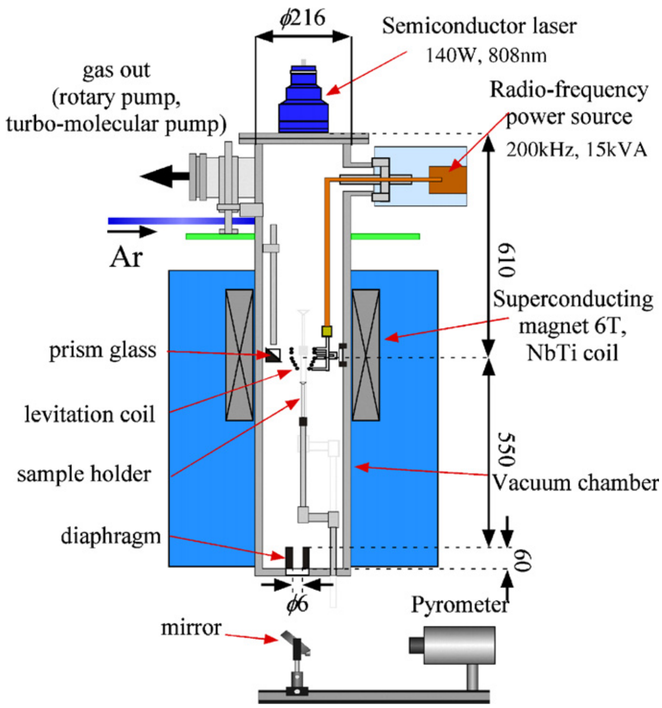

Fig. 1. A schematic diagram of the electromagnetic levitator developed to measure the thermal conductivity of molten silicon [18].

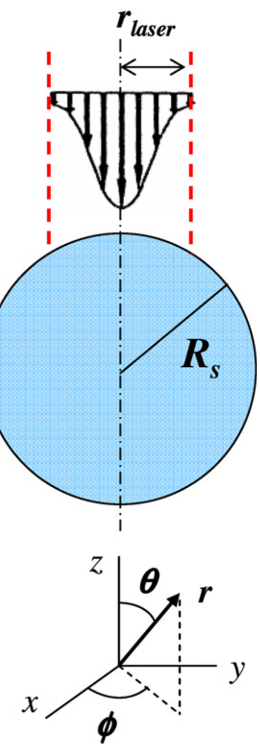

Fig. 2. A schematic diagram of a periodic laser-heating method.

source, i.e., a semiconductor laser in this work, and then the temperature variation at the lower part of the droplet caused by heat flow from the upper part through the droplet is detected by a pyrometer. In the experiment, the phase lag between the modulated light and the temperature variations detected by the pyrometer, $\Delta\phi_s$, is measured at various frequencies of the modulated light, ω, where $\Delta\phi_s$ depends on the thermal conductivity, emissivity and diameter of the droplet.

In the analysis of the temperature variations in an electromagnetically levitated droplet whose upper part is irradiated by a modulated light source, the following are assumed: (1) the system is axially symmetric, (2) the thermophysical properties of the droplet are constant, (3) the droplet is opaque to the light source, i.e., the light source is partially absorbed at the surface and the rest is reflected, (4) the distribution of laser intensity is Gaussian, (5) the heat loss from the droplet surface is radiation alone, and (6) the heat transfer in the droplet is governed by conduction alone, because convection in the droplet is completely suppressed by applying a static magnetic field.

Under the above assumptions, the unsteady-state heat conduction equation in the spherical coordinate system is expressed as follows:

$$\rho C_p \frac{\partial T}{\partial t} = k\left[\frac{1}{r^2}\frac{\partial}{\partial r}\left(r^2\frac{\partial T}{\partial r}\right) + \frac{1}{r^2\sin\theta}\frac{\partial}{\partial\theta}\left(\sin\theta\frac{\partial T}{\partial\theta}\right)\right] + Q(r,\theta) \tag{1}$$

where $Q(r,\theta)$ is the heat generation rate due to electromagnetically induction heating.

The boundary conditions are given by the following equations:

at the droplet surface irradiated by the laser:

$$-k\frac{\partial T}{\partial n} = \sigma_{SB}\varepsilon(T^4 - T_a^4) - \alpha I_0(t)\exp\left[-\frac{2R_s^2\sin^2\theta}{r_{laser}^2}\right](-\boldsymbol{n}\cdot\boldsymbol{e}_{laser}) \tag{2}$$

at the droplet surface without the light source:

$$-k\frac{\partial T}{\partial n} = \sigma_{SB}\varepsilon(T^4 - T_a^4) \tag{3}$$

at the centerline:

$$-k\frac{\partial T}{\partial\theta} = 0 \tag{4}$$

and the initial condition is as follows:

$$T = T_0(r,\theta) \tag{5}$$

Here, in Eq. (2), $\boldsymbol{n}$ is the unit normal vector at the droplet surface, $\boldsymbol{e}_{laser}$ is the unit vector pointing out the incident direction of the laser, and I_0 is the intensity of the laser beam at the centerline which is related to the power of the modulated laser beam, $P_0(\cos\omega t + 1)$, as follows:

$$I_0(t) = \frac{2}{\pi r_{laser}^2}P(t) = \frac{2}{\pi r_{laser}^2}P_0(\cos\omega t + 1) \tag{6}$$

In Eq. (5), $T_0(r,\theta)$ is the initial temperature distribution in the droplet just before laser heating, which is determined by considering the electromagnetically induced Joule heat.

2.2. Simplified model

Basically, the thermal conductivity and emissivity of the droplet may be determined by fitting the experimental temperature response detected by a pyrometer with the results obtained by solving numerically Eqs. (1)–(6) if the thermophysical properties other than these parameters, i.e., density and specific heat, are known. However, since Eq. (1) gives the unsteady-state solutions and the boundary conditions for radiation at the droplet surface, Eqs. (2) and (3), are nonlinear, it seems that they are too troublesome to use as the system of equations for determining the thermophysical properties. In addition, the ambient temperature T_a and $T_0(r,\theta)$ must be predetermined experimentally, but it is difficult to measure these values. Therefore, in the present analysis, Eqs. (1)–(6) are simplified as described below.

When the upper part of the droplet is irradiated by the modulated laser beam as shown in Fig. 2, the temperature at each point in the droplet, $T(r,\theta,t)$, exhibits increases in average temperature and modulation amplitude from the initial temperature, and then reaches the stationary modulation state with certain constant average temperature and amplitude, depending on the power and frequency of the laser beam. In the present analysis, we consider only the temperature response at the stationary modulation state, and express the temperature $T(r,\theta,t)$ as follows:

$$T(r,\theta,t) = T_0 + \Delta T_{av}(r,\theta) + \Delta T_{md}(r,\theta,t), \tag{7}$$

where $\Delta T_{av}(r,\theta)$ is the increase in average temperature and $\Delta T_{md}(r,\theta,t)$ is the modulation amplitude. In addition, the initial temperature T_0 is assumed to be uniform throughout the droplet. At the stationary modulation state where the temperature varies sinusoidally with time, $\Delta T_{md}(r,\theta,t)$ is expressed in the following form:

$$\Delta T_{md}(r,\theta,t) = \Delta T^{in}_{md}(r,\theta)\cos\omega t + \Delta T^{out}_{md}(r,\theta)\sin\omega t \tag{8}$$

where $\Delta T^{in}_{md}(r,\theta)$ and $\Delta T^{out}_{md}(r,\theta)$ are the in-phase and out-of-phase components of $\Delta T_{md}(r,\theta,t)$, respectively. Then, substituting Eqs. (7) and (8) into Eq. (1), the following steady-state linear equation systems for $\Delta T^{in}_{md}(r,\theta)$ and $\Delta T^{out}_{md}(r,\theta)$ are obtained

$$k\left[\frac{1}{r^2}\frac{\partial}{\partial r}\left(r^2\frac{\partial(\Delta T^{in}_{md})}{\partial r}\right) + \frac{1}{r^2\sin\theta}\frac{\partial}{\partial\theta}\left(\sin\theta\frac{\partial(\Delta T^{in}_{md})}{\partial\theta}\right)\right] - \rho C_p\omega\Delta T^{out}_{md} = 0 \tag{9}$$

$$k\left[\frac{1}{r^2}\frac{\partial}{\partial r}\left(r^2\frac{\partial(\Delta T^{out}_{md})}{\partial r}\right) + \frac{1}{r^2\sin\theta}\frac{\partial}{\partial\theta}\left(\sin\theta\frac{\partial(\Delta T^{out}_{md})}{\partial\theta}\right)\right] + \rho C_p\omega\Delta T^{in}_{md} = 0 \tag{10}$$

Additionally, assuming that the increases in both average temperature and modulation amplitude, $\Delta T_{av}(r,\theta)$ and $\Delta T_{md}(r,\theta,t)$, are much less than initial temperature T_0, i.e.,

$$(T_0 + \Delta T_{av} + \Delta T_{md})^4 \approx T_0^4\{1 + 4((\Delta T_{av} + \Delta T_{md})/T_0)\} \tag{11}$$

the boundary conditions for $\Delta T^{in}_{md}(r,\theta)$ and $\Delta T^{out}_{md}(r,\theta)$ are given by the following linear equations:

at the droplet surface irradiated by the laser:

$$-k\frac{\partial(\Delta T^{in}_{md})}{\partial n} = 4\sigma_{SB}\varepsilon T_0^3\Delta T^{in}_{md} - \frac{2\alpha P_0}{\pi r^2_{laser}}\exp\left[-\frac{2R_s^2\sin^2\theta}{r^2_{laser}}\right](-\boldsymbol{n}\cdot\boldsymbol{e}_{laser}) \tag{12}$$

$$-k\frac{\partial(\Delta T^{out}_{md})}{\partial n} = 4\sigma_{SB}\varepsilon T_0^3\Delta T^{out}_{md} \tag{13}$$

at the droplet surface without the light source:

$$-k\frac{\partial(\Delta T^{in}_{md})}{\partial n} = 4\sigma_{SB}\varepsilon T_0^3\Delta T^{in}_{md} \tag{14}$$

$$-k\frac{\partial(\Delta T^{out}_{md})}{\partial n} = 4\sigma_{SB}\varepsilon T_0^3\Delta T^{out}_{md} \tag{15}$$

at the centerline:

$$-\frac{\partial(\Delta T^{in}_{md})}{\partial\theta} = 0 \tag{16}$$

$$-\frac{\partial(\Delta T^{out}_{md})}{\partial\theta} = 0 \tag{17}$$

Eqs. (9) and (10) are solved with the boundary conditions equations (12)–(17) to determine the distributions of $\Delta T^{in}_{md}(r,\theta)$ and $\Delta T^{out}_{md}(r,\theta)$ in the droplet. Then, using $\Delta T^{in}_{md}(r,\theta)$ and $\Delta T^{out}_{md}(r,\theta)$, the distributions of the phase lag $\Delta\phi_s(r,\theta)$ in the droplet can be obtained with the following equation:

$$\Delta\phi_s(r,\theta) = \tan^{-1}\left(\frac{\Delta T^{out}_{md}}{\Delta T^{in}_{md}}\right) \tag{18}$$

2.3. Determination of thermal conductivity and emissivity

To determine simultaneously the thermal conductivity and emissivity of the droplet, the experimental results for $\Delta\phi_s$ at various frequencies of the modulated light ω are fitted with the numerical results obtained by the above-mentioned simplified model. Here, the finite element method was adopted to solve numerically Eqs. (9)–(17) for the droplet with arbitrary shape. The calculation domain is discretized by isoparametric nine-noded quadrilateral elements, and $\Delta T^{in}_{md}(r,\theta)$ and $\Delta T^{out}_{md}(r,\theta)$ are approximated with biquadratic interpolation functions. To fit the experimental values of phase lag $\Delta\phi_s$, the integral mean value of $\Delta\phi_s$ in Eq. (18) over the spot area of the pyrometer was evaluated using the following equation:

$$\Delta\phi_s = \tan^{-1}\left(\frac{\text{average}(\Delta T^{out}_{md})}{\text{average}(\Delta T^{in}_{md})}\right) \tag{19}$$

where

$$\mathrm{average}(\Delta T_{\mathrm{md}}^{\mathrm{in}}) = \frac{1}{S_{\mathrm{pyrometer}}}\int_S \Delta T_{\mathrm{md}}^{\mathrm{in}}(r,\theta) r \sin\theta \sqrt{(\mathrm{d}r)^2 + (r\mathrm{d}\theta)^2} \tag{20}$$

$$\mathrm{average}(\Delta T_{\mathrm{md}}^{\mathrm{out}}) = \frac{1}{S_{\mathrm{pyrometer}}}\int_S \Delta T_{\mathrm{md}}^{\mathrm{out}}(r,\theta) r \sin\theta \sqrt{(\mathrm{d}r)^2 + (r\mathrm{d}\theta)^2} \tag{21}$$

and $S_{\mathrm{pyrometer}}$ is the spot area of the pyrometer. The above numerical simulations are incorporated into the Levenberg–Marquardt method, which enables us to compute the nonlinear least squares solutions, as a model function, in order to determine simultaneously the thermal conductivity and emissivity of the molten droplet from the experimental relation between $\Delta\phi_{\mathrm{s}}$ and ω.

3. Verification of present model

Before the estimation of the thermal conductivity and emissivity of molten silicon using the above mathematical model, it is important to ascertain the reliability and accuracy of the model. Therefore, the virtual measurement of the properties was carried out by numerical simulation. Here, the electromagnetic field in the electromagnetic levitator shown in Fig. 3, which was actually used to measure the thermal conductivity and emissivity of molten silicon, was analyzed numerically by using the hybrid finite difference and boundary element methods [20]. Then, the temperature fields in the electromagnetically levitated silicon droplet during periodic laser-heating were obtained by solving Eq. (1) with the boundary conditions, Eqs. (2)–(4), using a control volume method. Fig. 4a shows the calculated temperature response at the lower part of the droplet, i.e., the integral mean value of temperature over the region corresponding to the spot area of the pyrometer, for $\omega/2\pi = 0.1$ Hz, and additionally Fig. 4b shows the temperature distributions in the droplet for (i) to (iv) in Fig. 4a. The physical properties of the molten silicon and processing parameters used in the calculations are listed in Table 1. From the figures, it can be seen that the isotherms in the droplet are affected by the electromagnetically induced heterogeneous heat.

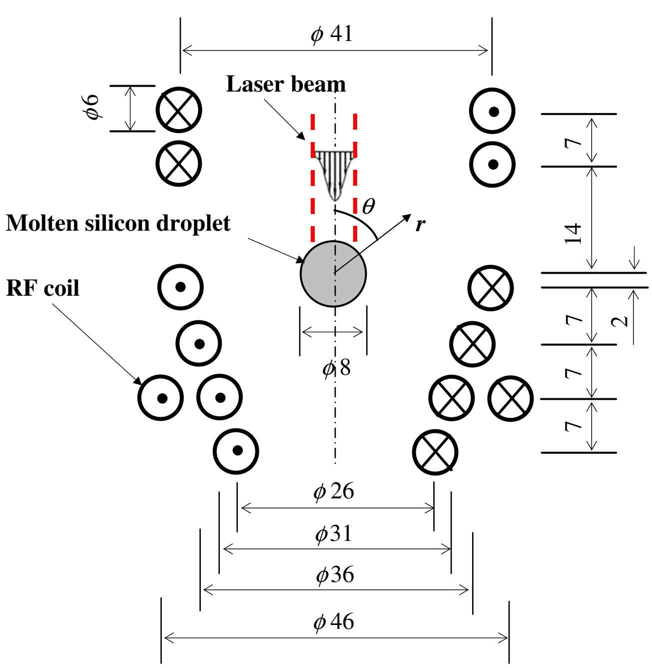

Fig. 3. Details of the geometry of RF coil in an electromagnetic levitator shown in Fig. 1.

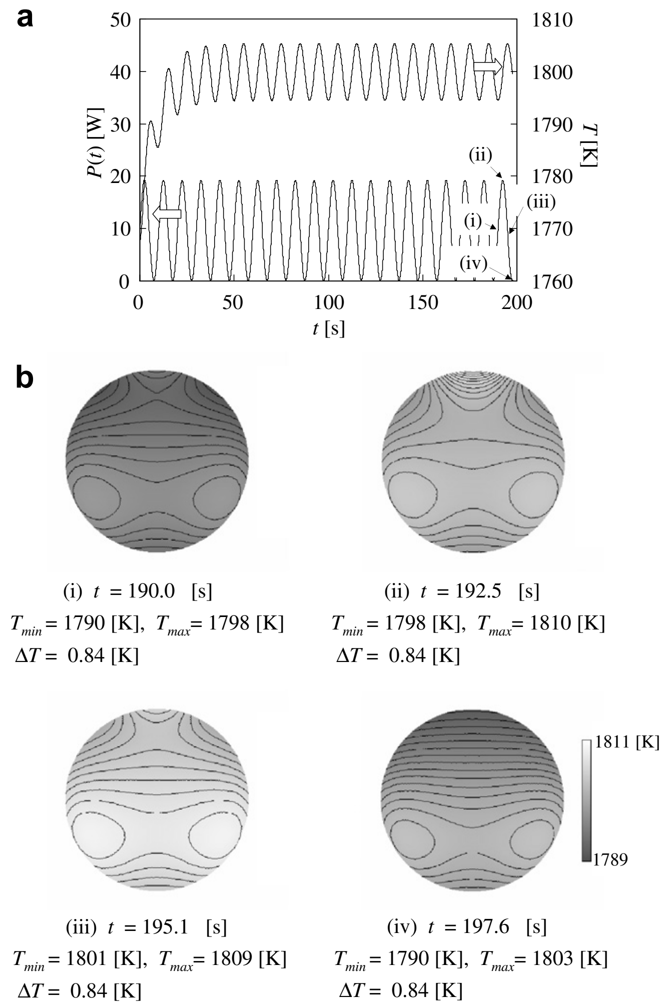

Fig. 4. (a) Calculated temperature responds at the lower part of the droplet. (b) Temperature distributions in the droplet.

Calculations similar to those in Fig. 4a were carried out by varying the frequency of the modulated laser beam ω. The plots in Fig. 5 show the relation between the phase lag $\Delta\phi_{\mathrm{s}}$ and ω calculated numerically. Then, the simplified mathematical model described in Section 2 was adopted to the plots in Fig. 5, as shown by a fitting line in the figure, and consequently the values 63.93 W/m K and 0.321 were obtained as thermal conductivity and emissivity, respectively. Comparing them with the input data in Table 1, the estimated value of thermal conductivity, 63.93 W/m K, is in good agreement with the input data, 64.00 W/m K, and it can be concluded that the present

Table 1
Physical properties and operating conditions used in calculations

Physical properties of molten silicon	
Density [kg/m^3]	2530
Thermal conductivity [W/(m K)]	64.0
Emissivity [–]	0.3
Specific heat [J/(kg K)]	1000
Electric conductivity [S/m]	1.2×10^6
Melting temperature [K]	1683
Operating conditions	
Electric current in RF coil [A]	375
Frequency of electric current in RF coil [kHz]	200
Laser power [W]	9.56
Ambient temperature [K]	323
Droplet diameter [m]	8×10^{-3}
e^{-2} radius of semiconductor laser beam [m]	2×10^{-3}
Spot radius of pyrometer [m]	2×10^{-3}

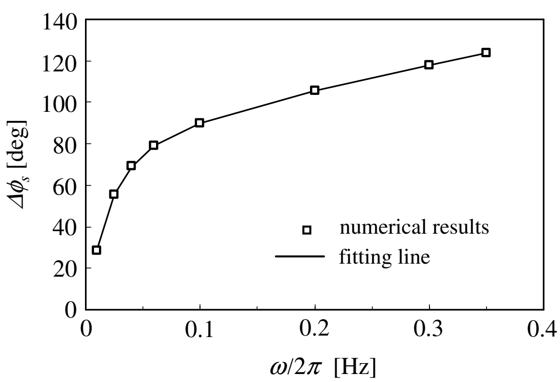

Fig. 5. Calculated relation between phase lag $\Delta\phi_s$ and frequency ω.

simplified model is appropriate for estimating the thermal conductivity of the electromagnetically levitated droplet. In addition, such agreement suggests that the electromagnetically induced heterogeneous thermal field in the droplet shown in Fig. 4b is not significant for the determination of thermal conductivity by the present model. On the other hand, the estimated value of emissivity, 0.321, is larger than that in Table 1, i.e., 0.3. The integral mean value of temperature over the region corresponding to the spot area of the pyrometer before being irradiated by a laser beam is 1768 K, and thus Eq. (11) is approximately satisfied. Therefore, it is inferred that the discrepancy between the estimated value and the emissivity in Table 1 is due to the fact that, actually, the initial temperature T_0 is not constant throughout the droplet.

4. Sensitivity analysis of thermophysical properties

Next, the sensitivity analyses of thermal conductivity and emissivity of molten silicon were carried out being based on the same numerical simulation as that in the previous section, where the effect of variations in these properties on the relation between $\Delta\phi_s$ and ω was investigated numerically. Fig. 6a and b show the calculated relations

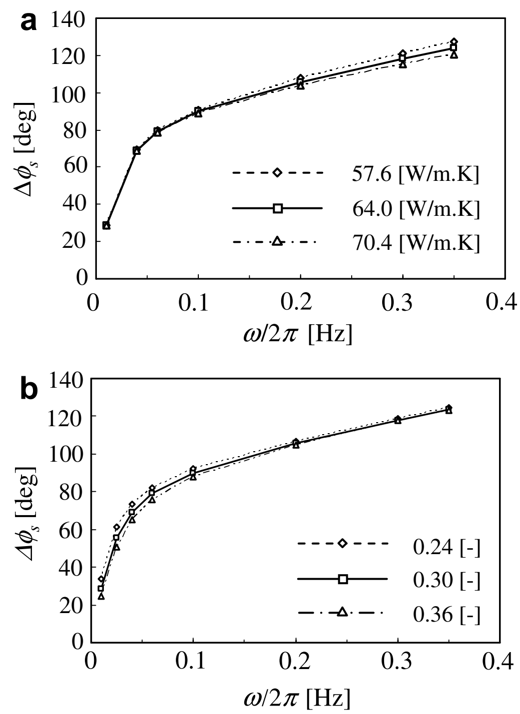

Fig. 6. Effect of variations in thermal conductivity and emissivity on the relation between $\Delta\phi_s$ and ω.

between $\Delta\phi_s$ and ω for three different values of thermal conductivity and emissivity, respectively, where the values in Table 1 were varied by ±10% for thermal conductivity and by ±20% for emissivity. In the calculations for emissivity, the initial temperatures in the droplet before laser-heating were equalized in all three cases by adjusting the value of the RF current. From the figure, it is found that the sensitivity of $\Delta\phi_s$ for thermal conductivity is significant over a wide range of frequency, while the sensitivity for emissivity becomes significant only at a much lower frequency, i.e., $\omega < 0.05$ Hz. Such an insensitivity of $\Delta\phi_s$ for emissivity was also reported by Wunderlich and Fecht [21], who measured the thermophysical properties of molten metal alloys by a modulated electromagnetic induction calorimetry. Consequently, it is suggested from Fig. 6 that the simultaneous determination of thermal conductivity and emissivity of molten silicon by the present model should be performed from the relation between $\Delta\phi_s$ and ω measured over a wide range of ω, particularly $\Delta\phi_s$ at low ω is essential for the precise determination of emissivity.

5. Measurement of thermal conductivity and emissivity of molten silicon

Fig. 7 shows the experimental relation between the phase lag $\Delta\phi_s$ and ω for a molten silicon droplet with a diameter of 8 mm obtained using the electromagnetic levitator shown in Fig. 1. Here, the upper part of an electromagnetically levitated silicon droplet was periodically heated by a semiconductor laser beam with a given

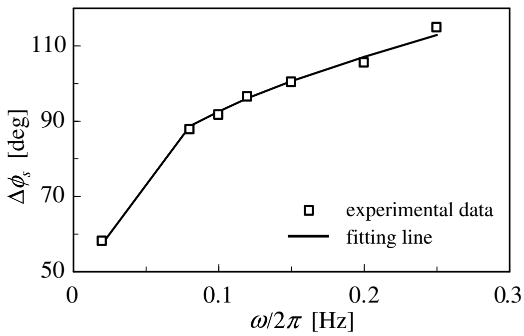

Fig. 7. Experimental relation between phase lag $\Delta\phi_s$ and frequency ω of molten silicon droplet.

frequency, and then the temperature variation at the lower part of the droplet was detected by a pyrometer, superimposing a static magnetic field of 4 T to suppress melt convection. The e^{-2} radius of the laser beam was 2.0 mm and the spot radius of the pyrometer was 2.0 mm. The measured values are shown by the plots in the figure, and then were fitted with the mathematical model described in Section 2, as shown by the solid line. Consequently, the values 67.6 W/m K and 0.23 were obtained as the thermal conductivity and emissivity of molten silicon at 1780 K, respectively, where the predetermined value 948 J/kg K was used as the specific heat of molten silicon [19], and the density was assumed to be 2446 kg/m^3, a literature value [12].

6. Conclusions

Recently, a novel method of measuring the thermophysical properties, especially thermal conductivity, of high-temperature molten droplets using the electromagnetic levitation technique has been developed by Fukuyama et al. [18,19], where the method was based on periodic laser-heating, and a static magnetic field was superimposed to suppress the melt convection in an electromagnetically levitated droplet. In the present work, the periodic laser-heating method was modeled to estimate the thermal conductivity and emissivity of the electromagnetically levitated droplet using a measured parameter, i.e., the phase lag between the modulated light and the temperature variations detected by a pyrometer, $\Delta\phi_s$, at various frequencies of the modulated light ω. Here, the unsteady-state heat conduction equation with radiative heat transfer to the ambient was simplified and transformed to the steady-state linear equations. The experimental relation between $\Delta\phi_s$ and ω was fitted by the mathematical model proposed here to estimate simultaneously the thermal conductivity and emissivity of molten silicon. Also, the numerical simulations for unsteady thermal field in the electromagnetically levitated droplet which was periodically laser-heated were carried out to demonstrate the validity of the proposed simplified model, and then to investigate the sensitivity of the thermophysical properties to the relation between $\Delta\phi_s$ and ω.

Acknowledgements

This study was subsidized by the Japan Keirin Association through its Promotion funds from KEIRIN RACE and was supported by the Mechanical Social Systems Foundation and the Ministry of Economy, Trade and Industry. The authors are grateful to Mr. C. Shimizu for his cooperation in the numerical simulations.

References

[1] D.P. Lukanin, V.V. Kalaev, Yu.N. Makarov, T. Wetzel, J. Virbulis, W. von Ammon, Advances in the simulation of heat transfer and prediction of the melt-crystal interface shape in silicon CZ growth, J. Cryst. Growth 266 (2004) 20–27.
[2] Th. Wetzel, J. Virbulis, A. Muiznieks, W. von Ammon, E. Tomzig, G. Raming, M. Weber, Prediction of the growth interface shape in industrial 300 mm CZ Si crystal growth, J. Cryst. Growth 266 (2004) 34–39.
[3] L.J. Liu, K. Kakimoto, Partly three-dimensional global modeling of a silicon Czochralski furnace. I. Principles, formulation and implementation of the model, Int. J. Heat Mass Transfer 48 (2005) 4481–4491.
[4] M. Przyborowski, T. Hibiya, M. Eguchi, I. Egry, Surface tension measurement of molten silicon by the oscillating drop method using electromagnetic levitation, J. Cryst. Growth 151 (1995) 60–65.
[5] W.K. Rhim, S.K. Chung, A.J. Rulison, R.E. Spjut, Measurements of thermophysical properties of molten silicon by a high-temperature electrostatic levitator, Int. J. Thermophys. 18 (1997) 459–469.
[6] M. Langen, T. Hibiya, M. Eguchi, I. Egry, Measurement of the density and the thermal expansion coefficient of molten silicon using electromagnetic levitation, J. Cryst. Growth 186 (1998) 550–556.
[7] H. Fujii, T. Matsumoto, N. Hata, T. Nakano, M. Kohno, K. Nogi, Surface tension of molten silicon measured by the electromagnetic levitation method under microgravity, Metall. Mater. Trans. A 31 (2000) 1585–1589.
[8] W.K. Rhim, K. Ohsaka, Thermophysical properties measurement of molten silicon by high-temperature electrostatic levitator: density, volume expansion, specific heat capacity, emissivity, surface tension and viscosity, J. Cryst. Growth 208 (2000) 313–321.
[9] H. Fujii, T. Matsumoto, K. Nogi, Analysis of surface oscillation of droplet under microgravity for the determination of its surface tension, Acta Mater. 48 (2000) 2933–2939.
[10] Z.H. Zhou, S. Mukherjee, W.K. Rhim, Measurement of thermophysical properties of molten silicon using an upgraded electrostatic levitator, J. Cryst. Growth 257 (2003) 350–358.
[11] Y.S. Sung, H. Takeya, K. Hirata, K. Togano, Specific heat capacity and hemispherical total emissivity of liquid Si measured in electrostatic levitation, Appl. Phys. Lett. 83 (2003) 1122–1124.
[12] K. Higuchi, K. Kimura, A. Mizuno, M. Watanabe, Y. Katayama, K. Kuribayashi, Precise measurement of density and structure of undercooled molten silicon by using synchrotron radiation combined with electromagnetic levitation technique, Measur. Sci. Technol. 16 (2005) 381–385.
[13] H. Kawamura, H. Fukuyama, M. Watanabe, T. Hibiya, Normal spectral emissivity of undercooled liquid silicon, Measur. Sci. Technol. 16 (2005) 386–393.
[14] J.H. Zong, B. Li, J. Szekely, The electromagnetic and hydrodynamic phenomena in magnetically-levitated molten droplets – I. Steady state behavior, Acta Astronautica 26 (1992) 435–449.
[15] B.Q. Li, S.P. Song, Thermal and fluid flow aspects of electromagnetic and electrostatic levitation – a comparative modeling study, Microgravity Sci. Technol. XI (1998) 134–143.
[16] V. Bojarevics, K. Pericleous, Modeling electromagnetically levitated liquid droplet, ISIJ 43 (2003) 890–898.
[17] R.W. Hyers, Fluid flow effects in levitated droplets, Measur. Sci. Technol. 16 (2005) 394–401.

[18] H. Fukuyama, H. Kobatake, I. Minato, K. Takahashi, T. Tsukada, S. Awaji, Establishment of noncontact AC calorimetry of high-temperature melts using solid platinum spheres as a reference, in: Proceeding of 16th Symposium on Thermophysical Properties, CD-ROM, 2006, p. 937.
[19] H. Kobatake, H. Fukuyama, I. Minato, T. Tsukada, S. Awaji, Noncontact AC calorimetry of liquid silicon with suppressing convections in a static magnetic field, in: Proceedings of 16th Symposium on Thermophysical Properties, CD-ROM, 2006, p. 625.
[20] A.F. Kolesnichenko, A.D. Podoltsev, I.N. Kucheryabaya, Action of pulse magnetic field on molten metal, ISIJ 34 (1994) 715–721.
[21] R.K. Wunderlich, H.-J. Fecht, Modulated electromagnetic induction calorimetry of reactive metallic liquids, Measur. Sci. Technol. 16 (2005) 402–416.